ALTERED EEG OSCILLATORY BRAIN NETWORKS DURING MUSIC-LISTENING IN MAJOR DEPRESSION

Yongjie Zhu[a, b, h, 1], Xiaoyu Wang[a], Klaus Mathiak[d], Petri Toiviainen[c], Tapani Ristaniemi[b], Jing Xu[e, 2 *], Yi Chang[e, 3 *], Fengyu Cong[a, b, f, g4 *]

[a] *School of Biomedical Engineering, Faculty of Electronic and Electrical Engineering, Dalian University of Technology, 116024, Dalian, China*

[b] *Faculty of Information Technology, University of Jyväskylä, 40014, Jyväskylä, Finland*

[c] *Department of Music, Art and Culture Studies, University of Jyväskylä, 40014, Jyväskylä, Finland*

[d] *Department of Psychiatry, Psychotherapy and Psychosomatics, Medical Faculty, RWTH Aachen, Pauwelsstraße 30, D-52074 Aachen, Germany*

[e] *Department of Neurology and Psychiatry, First Affiliated Hospital, Dalian Medical University, Dalian, China*

[f] *School of Artificial Intelligence, Faculty of Electronic Information and Electrical Engineering, Dalian University of Technology, Dalian, China*

[g] *Key Laboratory of Integrated Circuit and Biomedical Electronic System, Liaoning Province. Dalian University of Technology, Dalian, China*

[h] *Department of Computer Science, University of Helsinki, Helsinki, Finland*

[1] yongjie.zhu@foxmail.com

[2] xujing_doc@aliyun.com

[3] changee99@gmail.com

[4] cong@dlut.edu.cn

To examine the electrophysiological underpinnings of the functional networks involved in music listening, previous approaches based on spatial independent component analysis (ICA) have recently been used to ongoing electroencephalography (EEG) and magnetoencephalography (MEG). However, those studies focused on healthy subjects, and failed to examine the group-level comparisons during music listening. Here, we combined group-level spatial Fourier ICA with acoustic feature extraction, to enable group comparisons in frequency-specific brain networks of musical feature processing. It was then applied to healthy subjects and subjects with major depressive disorder (MDD). The music-induced oscillatory brain patterns were determined by permutation correlation analysis between individual time courses of Fourier-ICA components and musical features. We found that 1) three components, including a beta sensorimotor network, a beta auditory network and an alpha medial visual network, were involved in music processing among most healthy subjects; and that 2) one alpha lateral component located in the left angular gyrus was engaged in music perception in most individuals with MDD. The proposed method allowed the statistical group comparison, and we found that: 1) the alpha lateral component was activated more strongly in healthy subjects than in the MDD individuals, and that 2) the derived frequency-dependent networks of musical feature processing seemd to be altered in MDD participants compared to healthy subjects. The proposed pipeline appears to be valuable for studying disrupted brain oscillations in psychiatric disorders during naturalistic paradigms.

Keywords: Major depressive disorder; naturalistic music listening; ongoing EEG; independent component analysis; brain networks; neural oscillations.

1. Introduction

A number of robust brain networks have recently been revealed by neuroimaging tools [1, 2]. Those networks are thought to involve cognition and attention or reflect fundamental neural processes and dysfunctions in neurological and psychiatric disorders [3-7]. Most brain networks can be observed even during resting state and are therefore referred to as *resting state networks* (RSNs). The description of RSNs gives new insight into how separated brain regions dynamically integrate. One

* Corresponding authors.

of the RSNs, the default mode network, which is composed of brain areas demonstrating the greatest spontaneously metabolic activity at rest, has been assumed to reflect the brain's intrinsic default pattern [8, 9]. In addition to RSNs, some task-relevant transient networks related to self-paced movement, perception and working memory have been observed [10], where temporal courses of dynamic connectivity were analyzed based on envelope correlation with time-windowed data and between pairs of spatially separate regions defined by cortical segmentation [11, 12].

Recently, increased interest has been directed to exploring functional brain networks during natural paradigms such as music, movies, and video [13-18]. Unlike the repetitions of abstracted stimuli in order to improve the signal to noise ratio of recorded data [19-24], it is a challenge to uncover brain activity during naturalistic paradigms [25]. Nevertheless, many methods and techniques have been applied to explore the electrophysiological processes underlying naturalistic stimuli. Inter-subject correlation approaches have been used to show inter-subject synchronization during natural viewing in *functional magnetic resonance imaging* (fMRI) [26], *magnetoencephalography* (MEG) [27] and *electroencephalography* (EEG) [28]. By combining fMRI, computational acoustic feature extraction and behavioral psychology, Alluri et al. found that large-scale brain networks emerged when participants freely listened to music [13]. Zhu et al. recently combined acoustic feature extraction, spatial Fourier *independent component analysis* (ICA) and clustering to examine the frequency-specific brain networks involved in music listening in healthy participants, which demonstrated that functional brain patterns for processing of musical feature are frequency-specific [29]. These findings also demonstrated common spatio-spectral patterns (frequency-specific bran networks) are similar across participants under music listening.

Major depressive disorder (MDD), is a mental disorder characterized by low mood, loss of interest in normally enjoyable activities, and low self-esteem, as well as cognitive impairment, psychomotor agitation, and functional impairment [30]. Treatment for MDD is usually inadequate, and the underlying mechanisms of such disease are not well understood [31]. Within the last decade, a number of neuroimaging studies using different methodologies have demonstrated that MDD is related to altered brain network function [32-38]. Altered brain networks were observed across those coordinating interactions between several spatially separate brain regions supporting multiple specific cognitive functions, such as emotion, attention and self-referential processing. Moreover, the neuropathology of MDD is associated with altered connections between different brain systems [39]. Even though findings concerning altered neural, connections within and between these networks vary among studies, it is argued that MDD can be understood as a "network disease" with pathological changes in functional connectivity patterns [40]. Also, some studies explored music listening as a potential complementary intervention to reduce depressive symptoms, which demonstrated that music could be offered as a way to help patients reduce anxiety [41-43]. Yet, the neurobiological mechanisms underlying symptom improvement in depression during music listening remain unclear.

Up to now, many group comparison studies using group-level methods of resting state data have been reported across many pathologies [44, 45]. Nugent et al. performed group ICA on the Hilbert envelope of MEG data in MDD and healthy control groups to investigate group differences in RSNs [45]. In contrast, studies applying ICA techniques to brain data under naturalistic stimuli have investigated only healthy participants. For example, individual-level spatial Fourier ICA was successfully applied to ongoing EEG of healthy subjects while they freely listened to music in our previous study, which demonstrated that there are similar frequency-specific networks emerging across healthy subjects under music listening [29]. Few studies have attempted to investigate the differences in brain networks under naturalistic stimuli between healthy control subjects and MDD participants. Here, we present an approach that extends the individual analysis and allows us to examine group-level comparisons between a sample of healthy control participants and MDD participants while freely listening to music. We expected to see different frequency-specific networks of music processing in MDD subjects compared to healthy subjects. Additionally, we expected to find a plausible relationship between frequency-specific networks and depressive symptoms, as evaluated in clinical samples through depression questionnaire ratings.

2. Material and methods

Figure 1 demonstrated the analysis pipeline and we here introduced the overview. Two stages were performed in the proposed approach. In the individual-level stage, *short-time Fourier transform* (STFT) was performed on EEG data collected during music listening from MDD participants and healthy controls. A three-way array of data (time × frequency × channel) for each subject was obtained, and cortical source data were obtained via source localization based on minimum

norm estimation. The cortical three-way array was then reshaped into a two-way matrix (time × frequency ∗ channel) for each subject. In the group-level stage, the individual matrix from each subject was temporally concatenated since we assume that subjects shared the spatial profiles. The Fourier ICA was applied to obtain independent components including spatio-spectral factors and the temporal courses. The temporal courses were segmented into separate epochs, each of which was corresponding to an individual participant. Five musical (tonal and rhythmic) features were then extracted from the music stimuli. Finally, statistical analysis was performed to find music-induced brain activity in each group by correlating the time courses with musical feature time serials, and the components showing differences between groups were retained for further analysis. In addition, we also investigated the relationship between the activation strength of frequency-specific networks and depressive symptoms, as measured by questionnaire ratings of depression.

2.1. *Data description*

2.1.1. *Participants*

There were 20 psychiatrically healthy adults (4 males; 16 females) and 20 MDD adults (6 males; 14 females) in the current study. The mental health of each subjects was evaluated through the Structured Clinical Interview for DSM-IV-TR (SCID) and unstructured interviews with a psychiatrist. The *Hamilton Rating Scale for Depression* (HRSD), *Hamilton Anxiety Rating Scale* (HAMA), and *Mini-Mental State Examination* (MMSE) were used in the mental assessment. The HRSD is a multi-item questionnaire adopted to provide an indication of depression, and as a guide to assess recovery. The HAMA is a psychological questionnaire adopted by clinicians to assess the severity of a depressed patient's anxiety. The MMSE is a 5-minute bedside test that is used as a screen of mental status and to evaluate the degree of cognitive dysfunction in patients with diffuse brain disorders. The values of those indexes from all participants are listed in Table 1. The experimental procedure in this study was approved by the research ethics committee of the Dalian University of Technology and all the participants were informed about the experiment and have signed an informed written consent before participation.

2.1.2. *Stimulus*

The music clip adopted in the current experiment was the tango "Adios Nonino,", which has a duration of 8 minutes and 32 seconds. This music clip had been used in previous studies [46, 47] for its suitable length and high variance in several acoustical musical features such as tonality and rhythm.

Table 1. Demographic information of the participants.

	Controls (CON)		Patients with MDD		CON · MDD
	Mean (SD)	n	Mean (SD)	n	p values
Age, years	37.8 (11.4)	20	42.8 (10.7)	20	0.17
Gender (M:F)	4:16		6:14		0.96
Education (EDU)	13.7 (3.6)	20	12.8 (3.3)	20	0.40
HRSD	2.4 (1.2)	20	23.3 (3.5)	20	< 0.001
HAMA	2.3 (1.3)	20	19.2 (3.0)	20	< 0.001
MMSE	28.3 (0.9)	20	28.1 (1.0)	20	0.53
Duration of disease, months	-	-	12.8 (8.3)	20	-

Notes: M, male; F, female; HRSD, Hamilton Rating Scale for Depression; HAMA, Hamilton Anxiety Rating Scale; MMSE, Mini-Mental State Examination

2.1.3. *EEG recording*

The EEG measurements were conducted according to the International 10-20 system with 64 electrodes. The signals were amplified using Neuroscan amplifiers and sampled at a rate of 1,000 Hz. During the EEG measurements, subjects were asked to listen to music clip with their eyes open. Electrode impedances were kept below 5 KΩ. Common average channels were used to re-reference EEG data. Artifacts were corrected using infomax ICA in EEGLab toolbox [48]. A 50 Hz notch

filter, 1 Hz high-pass and 40 Hz low-pass filters were used to reduce noise. The EEG data were then downsampled to 256 Hz.

2.1.4. *Acoustic feature processing*

We extracted the musical features using the computational extraction approach adopted in previous studies [46, 47]. Five long-term musical features, including Fluctuation Centroid, Fluctuation Entropy, Key Clarity, Mode, and Pulse Clarity, were obtained from the musical stimuli using the *Music Information Retrieval* (MIR) Toolbox [49], which captures tonal and rhythmical properties. In brief, Fluctuation Centroid yields an estimate of the rate of musical events in the music; Fluctuation Entropy provides a measure of rhythmic complexity; Key Clarity indicates the degree to which the music

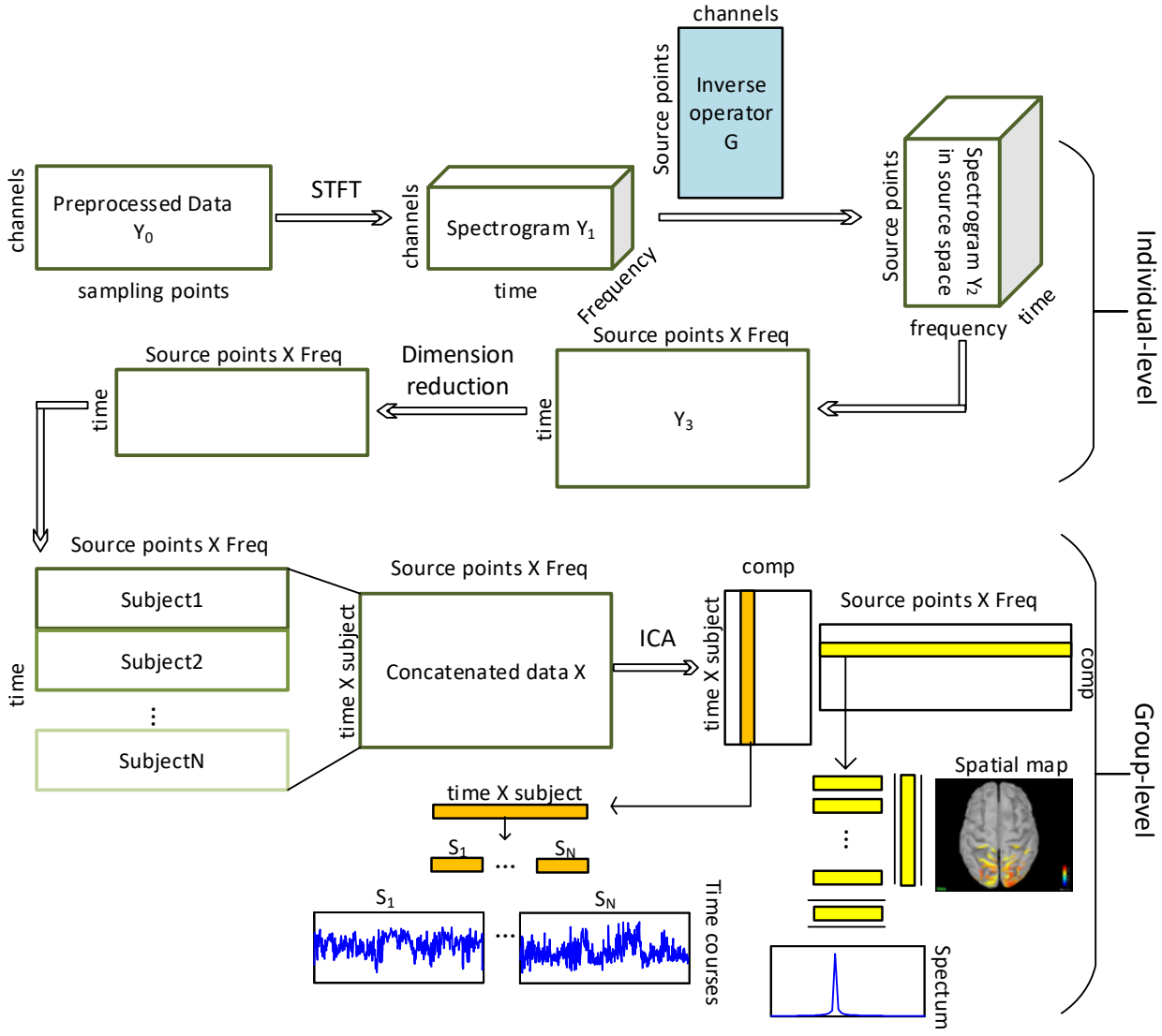

Fig. 1. Pipeline of group source-space ICA. At the individual-level stage, STFT was performed on the EEG data $\boldsymbol{Y_0}$ (N_c channel x N_p time point) to extract spectrogram data $\boldsymbol{Y_1}$ (N_c, N_f, N_t). The inverse operator $\mathbf{G}$ (see the main text) was left-multiplied to sensor-level data $\boldsymbol{Y_1}$ to obtain the spectrogram data $\boldsymbol{Y_2}$ (N_s,N_f,N_t) in source space. The three-order data $\boldsymbol{Y_2}$ was reshaped to the matrix $\boldsymbol{Y_2}$ (N_t, $N_s \times N_f$). Dimension reduction was performed using PCA subject by subject. At the group-level stage, reduced data were temporal concatenated to matrix $\boldsymbol{X_0}$. ICA decomposition was performed on this matrix. The columns of the mixing matrix represent the temporal courses of spatio-spectral patterns and the rows of independent source-level matrix were divided into the spatial maps and the corresponding spectra.

conforms with Western tonality structure; Mode indicates whether the music is in a major or minor key; and Pulse Clarity estimates the salience of a regular pulse in the music. We adopted a frame-by-frame analytical procedure used in the MIR field to extract musical features. We set the length of frames to 3-s and the adjacent overlap to 2 s (see [46], for the details). For each feature, this process yielded a time series with a 1 Hz sampling rate representing its temporal evolution. All processes were performed in the MATLAB environment.

2.2. *Group source-space ICA*

2.2.1. *Source analysis*

First, STFT (3s time window, 2s overlap and Hamming window) was applied to the preprocessed EEG data Y_0 (N_c channels x N_p sampling points) in the sensor space to obtain the corresponding spectrogram Y_1 (N_c,N_f,N_t). For each participant, the brain surface was reconstructed from an anatomical MRI template mesh, based upon the Montreal Neurological Institute human brain in Brainstorm [50]. Individual electrode positions of each EEG dataset were co-registered with the brain template based upon the three fiduciary points and electrode locations. At cortically separate constrained discrete locations (source points), we estimated the dipolar current sources. Each cerebral hemisphere was modeled by a cortical surface of around 2,000 source points (vertices), resulting in a mesh-grid of around 4,000 vertices modeling the brain surface for each participant. A single-compartment boundary element model (BEM) was used to model the conductivity of the cranium. The linear inverse operator G with dimension $N_s \times N_c$ (N_s denotes the number of vertices and N_c denotes the number of channels:$N_s \gg N_c$) was calculated using MNE with a loose orientation constraint favoring source currents perpendicular to the local cortical surface by a factor of 2.5 with respect to the currents along the surface in Brainstorm Toolbox. The spectrogram data Y_2 (N_s, N_t, N_f) at the cortical level was produced by left-multiplying the inverse operator matrix G (N_s, N_c) to the sensor-space matrix Y_1 (see Fig. 1).

2.2.2. *Group ICA*

After source localization, we reorganized the three-way array data Y_2 into two-way array Y_3 ($N_t, N_s \times N_f$). In the obtained matrix Y_3, its rows consisted of the STFT coefficient from each cortical voxel for the corresponding time point, and its columns comprised a time stamp corresponding to a time window in a specific frequency bin and source point. We performed PCA to reduce the dimension of the matrix Y_3 and whiten them. The selection of PCA dimensions was based upon fMRI studies [51] suggesting that the choice of dimensions was slightly greater than the expected number of underlying oscillatory sources. It has been suggested that 10–12 resting-state networks can be identified from the brain cortex using ICA with a model order around 25–40 dimensions [52]. Although there are information theoretic methods (e.g., AIC and BIC), such empirical rules appear to be more commonly used during dimensional reduction of neuroimaging data [52, 53]. In this study, we assume the number of the underlying sources to be 25 and set the order to 40. It should be noted that the above analysis was performed at the individual level. Then the reduced data from all subjects were concatenated in time domain. Temporal concatenation does not require the consistency across all subjects in time dimension for group ICA. It is required that all subjects share the spatio-spectral pattern. The consistency of spatio-spectral profiles (frequency-specific networks) was examined across subjects during music listening in our previous study [29]. The general issue of the spatial consistency assumption under the inter-subject differences has already been discussed in the related literature [54], and we will discuss this further below (see Discussion). We reduced the concatenated data to 40 dimensions at the group level. The spatial ICA was performed to estimate 25 underlying *independent components* (ICs) using fastICA in the MATLAB environment. The estimation of ICA maximized the independence in the spatial-spectral domain at the same time and the recovered spatial spectral ICs were independent with no requirement of temporal independence. The rows of the extracted component matrix S represent the independent spatio-spectral profiles, which were transformed to spatial maps and power spectrum by extracting the absolute value and by averaging across cortical points and frequency bins, separately. The absolute value of the column of the obtained mixing matrix A represents the temporal course corresponding to the independent spatio-spectral pattern. The details and interpretation can be found in previous studies [55, 56]. Fig. 1 demonstrates the flow chart with data matrix representation.

Since ICA estimation is not stable and depends on the randomly initialized procedure, there may be slight but quantifiable fluctuations in the resulting ICs among different runs. In the preliminary analysis, we noted that these fluctuations may cause small differences in group level results. To investigate the stability of ICA estimate, we used a well-developed Icasso toolbox [57]. This tool has already been adopted to assess stability among repeated runs of the fast-ICA algorithm and get more precise ICA estimations than any single ICA decomposition. All the ICs obtained from all ICA estimates were clustered using the absolute values of the correlation coefficient in the squared estimated sources. Then, the stability index, referred to as Iq, was calculated for each IC. Iq index represents the compactness and isolation of a cluster. Iq can be computed as:

$$Iq = \bar{S}(i)_{int} - \bar{S}(i)_{ext}\,,\ \ i = 1, \dots, J\,, \qquad (1)$$

where $\bar{S}(i)_{int}$ represents the averaged similarity of intra-cluster and $\bar{S}(i)_{ext}$ denotes the averaged similarity of inter-cluster. J indicates the underlying number of clusters. Note that the range of Iq is 0 to 1. Larger Iq means that the estimated ICs from all runs are more stable. In other words, if all the component clusters were separated from each other, the current ICA estimate were supposed to be stable. In general, ICA decomposition is considered to be stable if the Iq index is larger than 0.7.

The resulted ICs are spatio-spectral profiles. In order to obtain group level spatial maps and spectra for each IC, a matrix (N_f, N_s) in the spatio-spectral domain was obtained by rearranging each row of S, which means that a Fourier coefficient spectrum existed for each cortical source point. The spatial map (profile) was obtained by computing the average of the squared magnitude of the Fourier coefficient across those frequency bins satisfied with the top 5% squared Fourier amplitude. Similarly, the power spectrum of each IC was obtained by calculating the average of the Fourier power spectra across those source points satisfied with the 5% squared Fourier amplitude. Finally, the column of the mixing matrix A was considered as the concatenated time course across subjects, corresponding to the row of the estimated IC. The concatenated time courses were divided into individual segments, each of which corresponded to a single subject. After the back projection of PCA, the individual time courses of each participant were obtained for each ICs. Thus, we had N (number of subjects) time courses, a spatial map and a spectrum for each IC. The time courses reflect the temporal evolution of the spectro-spatial patterns.

2.2.3. *Components related to music-induced activity*

After ICA estimation, we obtained 25 ICs. The challenge was how to separate music-induced brain oscillations from spontaneous oscillations. In this study, we calculated Pearson's correlation coefficient between the musical feature time series and the individual temporal courses of the ICs. The permutation tests and Monte Carlo procedure presented in our previous work [46, 47] were applied to compute the threshold of the significant correlation coefficient for multiple comparisons. Then we counted the number of subjects whose time course was significantly correlated with music features in each group (CON and MDD) for every IC. If the number of subjects with significantly correlated time courses was more than half of participants for one IC, it was concluded that the IC reflected the brain activity linked to music stimuli across most participants in one specific group, and it was considered as a component associated with this group.

2.2.4. *Group differences between components*

For each IC, the variance of individual time courses was computed and used as a magnitude of activation for each participant. This magnitude can be considered an activation index of the spatio-spectral pattern (frequency-dependent network) during the whole duration of music listening. Thus, each subject had an activation index representing the activation magnitude of the spatio-spectral pattern for each IC. An one-factor (group) statistical analysis was performed to examine the group difference in the activation index for each IC. We demonstrated the group difference with a boxplot (see Fig. 3E). The ICs with activation p-value smaller than 0.05 were considered candidate ICs for further analysis. It should be noted that Bonferroni correction was used for p-values to correct for multiple comparisons across components.

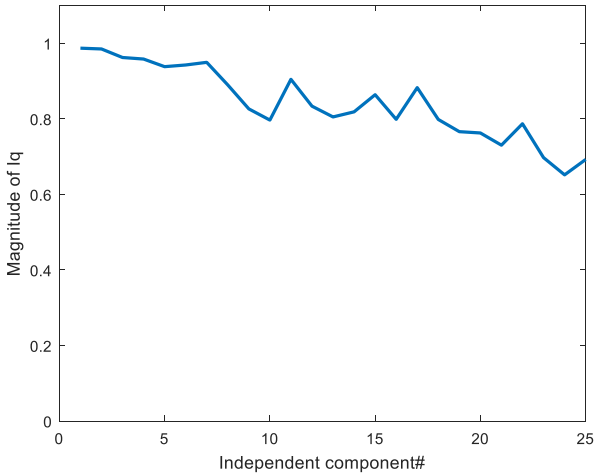

Fig. 2. Iq of each extracted component.

2.2.5. *Correlation between components and behavioral features*

Modulation in the power amplitude of neuronal oscillations has been functionally related to sensory, motor and cognitive function. Such relationship is commonly established by linking the power modulations to specific target variables such as task ratings or personality [58]. In this study, we examined the amplitude modulation of the frequency-dependent networks by the factors representing depressive symptoms via correlating the activation index with the behavioral data. Each subject had one activation index (see the section 2.2.4) and a behavioral scale index (e.g., the HAMA). For each IC, we computed the correlation coefficients between activation index sequences with behavioral index sequences in each group respectively. The threshold of significant correlation coefficient was obtained using the above procedure (see the section 2.2.3). If the activation index sequences in one of the groups were significantly correlated with one of the behavioral indexes for each IC, we considered this IC to be a candidate IC reflecting modulation by behavior for further analysis.

3. Results

3.1. Time series of *musical Features*

We extracted five long-term musical features using MIRtoolbox [49] with 3 seconds time window and 2 seconds overlap, yielding 1 Hz sampling rate of time courses. They include two tonal features, Mode and Key Clarity, and three rhythmic features, Fluctuation Centroid, Fluctuation Entropy, and Pulse Clarity. The time courses of these five features have 512 samples with 1Hz sampling rate, which could match the size and sampling rate of the temporal courses of the ICs extracted from EEG. We correlated those time series of musical features with the temporal courses of the extracted components to select the music-induced components.

3.2. *Stability analysis of ICA decomposition*

25 ICs were extracted by Icasso with 100 repeated runs for the concatenated data and calculated the stability index Iq according to Eq. 1. Fig. 2 demonstrates the magnitudes of Iq, larger than 0.7 for the majority of ICs. The 25 ICs were isolated from each other from the viewpoint of cluster. Hence, the ICA decomposition was reliable and the estimated results in the current study could be considered for further analysis.

3.3. *Notable components from ICA decomposition*

After 25 ICs derived from combined group data, we visualized the spatial profile, spectral profile, the number of subjects whose time courses were associated with the time courses of each musical feature in each group, the correlation of behavioral data (depressive symptoms) and the activation magnitude differences between groups for each IC. Fig. 3 demonstrates seven ICs showing group difference between CON and MDD group.

3.3.1. *Components associated with the CON group*

We found one unilateral auditory component at ~20 Hz (see Fig. 3 I). In the control group there were 12 subjects whose temporal courses were significantly correlated with musical features and 5 subjects whose temporal courses were significantly correlated with musical features in the MDD group, suggesting this ~20 Hz auditory network in healthy subjects is more engaged in musical feature processing than in the participants with MDD. No significant correlations between the activation magnitudes with behavioral data were observed in either group. There was also no significant difference between the two groups about the activation index. A bilateral 15 Hz sensorimotor component was found (see Fig. 3 II), which has been previously observed with fMRI of healthy subjects listening to music [46]. In the control group, 11 subjects' temporal courses were associated with stimuli features; in the MDD group the temporal courses of eight subjects were associated with stimuli features. The activation strength of the MDD group was significantly correlated with HAMA scores. We also found a unilateral visual component at ~10 Hz (Fig. 3 III). There were 11 control subjects and 5 MDD subjects whose temporal courses were significantly correlated with musical features. The statistical analysis revealed no significant difference between the two groups. Also, this component was unrelated to the behavioral scores.

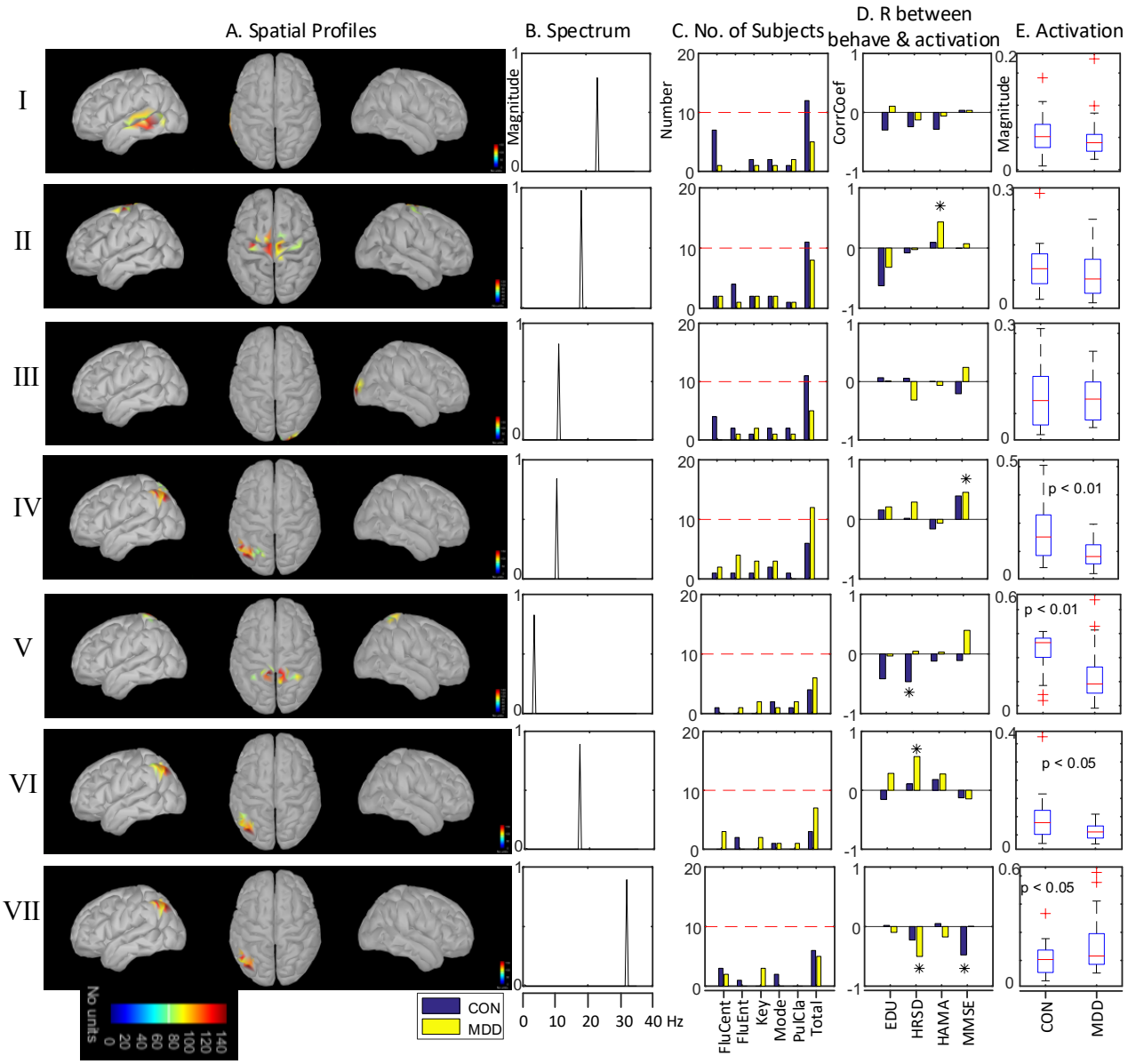

Fig. 3. A. Spatial map averaging the independent component across the Fourier bins; B. Spectra averaging the independent component across source points exceeding the 95th percentile threshold; C. Number of subjects whose temporal courses significantly correlated with musical features; D. Correlation coefficient between the variance of time courses with behavioral features (asterisk reflects significant correlation). E. Differences in activation strength between control and MDD groups.

3.3.2. *Components associated with the MDD group*

A unilateral lateral visual component (located in the left angular gyrus) at ~10 Hz (Fig. 3 IV) was found. There were 11 subjects with MDD and 6 healthy subjects in the control group whose time courses significantly correlated with musical features. Moreover, the activation magnitude of subjects with MDD was significantly correlated with cognitive score (quantified by the MMSE) and smaller than the activation magnitude of healthy subjects ($p < 0.01$).

3.3.3. *Components with a significant difference between groups*

A unilateral lateral visual component (located in the left angular gyrus) at ~10 Hz. We also found a sensorimotor component at ~ 5 Hz and two lateral visual components at ~15 Hz and ~ 30 Hz respectively (Fig. 3 V, VI&VII). For these components, the number of participants showing temporal courses significantly correlated with the musical features was less than half of the participants in both groups. The power of the ~5 Hz sensorimotor (located in the postcentral gyrus) component in the control group was negatively correlated with HSRD score. The activation of this network in the control group was stronger than the activation in MDD group ($p < 0.01$) (Fig. 3 V). The amplitude of the ~15 Hz lateral visual network component (located in left angular gyrus) of the MDD group was positively correlated with HSRD score. There was a significant difference in the activation of the networks between groups ($p < 0.05$; Fig. 3 VI). For the ~30 Hz lateral visual network component (also located in the left angular gyrus), the power of the subjects with MDD was negatively correlated with HRSD score. The power of the healthy subjects was negatively correlated with MMSE. The average activation of the subjects with MDD was stronger than that of the healthy subjects (Fig. 3 VII).

4. Discussion

In this study, we investigated group differences in frequency-specific brain patterns during music listening between participants with MDD and healthy controls using a technique combining group-level spatial Fourier ICA and acoustic feature extraction. The spatial Fourier ICA was used to extract independent spatio-spectral profiles. The individual temporal courses of the frequency-dependent networks were obtained by dividing the row of mixing matrix into *N* (number of subjects) segments. Then, musical features were extracted by music information retrieval. Music-induced frequency-specific networks for each group were identified by correlating temporal courses of spatio-spectral patterns with time series of the musical features. We further examined between group differences of network activation magnitude via statistical analysis and analyzed how magnitudes of networks were modulated by behavioral factors (specifically, depressive symptoms). The applied spatial Fourier ICA technique was first presented by Ramkumar and colleagues [55], which was able to capture the interactions between spatial profiles and spectral band. Shortly thereafter, a group-level spatial ICA was performed on a single healthy group of subjects to probe resting-state spatio-spectral patterns [56]. Recently, Zhu et al. also applied individual spatial Fourier ICA to the ongoing EEG of healthy subjects during music listening and found the brain networks of music processing to be frequency-dependent [29]. For spatial Fourier ICA, the meaning of independence is different from the meaning of independence in standard spatial ICA as used in fMRI [56] or as a feature extractor [59]. In spatial ICA, the independent components should be a set of statistically independent spatial maps together with similar temporal courses. Likewise, in spatial Fourier ICA, the estimated components should be independent in the spatio-spectral domain. This means that two components might be strongly overlapping in spatial domain, if they have very different, completely non-overlapping spectral profiles; the theoretical details can be found in previous studies [55, 56]. Until now, studies using this spatial Fourier ICA approach have focused on a single group of healthy subjects, and no studies have yet been presented for group comparisons under naturalistic music listening. We extended the spatial Fourier ICA to enable group comparisons under music listening and demonstrated the technique in a sample of subjects with MDD. In addition, the stability of the decomposition was examined by a well characterized tool, Icasso [57]. Nugent et al. also developed a MEG-ICA technique to examine the group-level differences in resting-state networks in subjects with MDD, which only investigated the beta frequency band [60].

We applied the proposed method to a group of 20 subjects with MDD under a music listening condition. We observed a ~20 Hz unilateral auditory component, a ~15 Hz bilateral sensorimotor component, and a ~10 Hz medial visual component associated with music processing among most healthy controls (see Fig. 3 I, II&III). The ~20 Hz unilateral auditory component and ~10 Hz medial visual component are in line with our previous work where the individual-level spatial ICA was performed to analyze electrophysiological networks of healthy subjects during a similar music listening condition [29]. The ~15 Hz bilateral sensorimotor component emerged in the current group-level analysis. Those brain networks seem to be more involved in music processing in healthy subjects than in patients with MDD. In other words, these spatial spectral patterns of MDD patients were not sensitive to natural music due to the severity of self-focused rumination in depressive patients. MDD has been linked to the predominance of default mode network over the task positive network, which is considered as a neurobiological basis for ruminative responding and multiple studies have

explored the depression-related changes in oscillatory brain activity [61-63]. Functional magnetic resonance imaging (fMRI) uncovered a modification in the functioning of frontal and temporal regions [64]. In addition, the magnitude of activation of the ~15 Hz bilateral sensorimotor component was modulated by anxiety score in the MDD group, seemingly indicating that depressive symptoms were associated with altered sensorimotor areas at the beta frequency band. Those results were consistent with earlier studies, demonstrating that depressive symptoms were associated with electrophysiological changes. In the resting state condition, major depression disorder was characterized by unique EEG rhythm in beta frequencies that were dominant in relation to delta, theta, and alpha oscillations and beta oscillations were associated with higher cognitive systems [65].

The ~10 Hz temporo-occipital component with spatial maxima over the left angular gyrus was engaged in music processing among most subjects with MDD (see Fig. 3 IV). The activation magnitude of this pattern was modulated by cognitive score in MDD subjects. Furthermore, the activation magnitude in the control group was significantly stronger than in the MDD group ($p < 0.01$). Previous studies demonstrated that connectivity of the temporal cortex centered in the precentral and angular gyri was increased in the MDD group [60]. In contrast, in the current study, the activation magnitude of the angular gyri was weaker in MDD participants. Alpha power in the left hemisphere was significantly larger than in the right. This alpha asymmetry was related to depressive mood, which corresponds to findings from an earlier study [66].

The activation magnitude of the ~5 Hz sensorimotor network was larger in the control group than in the MDD group ($p <0.001$). A ~15 Hz and ~30 Hz temporo-occipital components were both examined. The magnitude of the ~15 Hz temporo-occipital network was positively correlated with HRSD depressive symptoms in the MDD group and was weaker than in the control group. In contrast, the activation magnitude of the ~30 Hz network was positively correlated with HRSD depressive symptom and was larger than in the CON group. Although the brain areas are the same in both components, the spectral peak is different. These results suggest that MDD is associated with disrupted oscillatory brain networks (see review by [67]).

In all group ICA-based methods, a general question is which dimension is consistent across subjects and should be concatenated. In our previous work, we applied individual spatial Fourier ICA to ongoing EEG under a music listening condition; the common patterns in spectro-spatial domain were confirmed across healthy subjects but temporal courses were quite different among subjects [29]. In addition, Nugent et al. applied group-level MEG-ICA techniques to patients with MDD and heathy subjects to examine group difference in connectivity, where temporal concatenation in group ICA was performed and all subjects shared the same mixing matrix in spatial dimension [60]. Thus, those prior works motivated us to adopt a standard approach of temporal concatenation across subjects to organize the group data, which imposes a degree of spectro-spatial consistency due to the shared components in the spectro-spatial domain. Generally, concatenation in time dimension might result in spurious correlations in the data. Despite the fact that we are not aware of any study that has shown such spurious correlations (whether linear or nonlinear) in the context of group-level ICA, such a possibility could not be completely ruled out [56]. Moreover, the three-way tensor data were rearranged into a two-way matrix to facilitate ICA estimation, which may inevitably lose some potentially existing interactions between the spatial mode and the spectral mode. In the future, we would apply tensor decomposition to probe the underling interactions among multiple modes of the tensor [68-70]. We here used the tango Adios Nonino by Astor Piazzolla since dynamic functional networks during this piece of music listening are well described using healthy subjects in our previous studies [46, 47], where the spatial or temporal patterns of brain activity during listening to this music are synchronized participants. Another limitation of the current study is that a template head model was adopted for co-registration instead of individual MRI-derived head shape models. Due to the measurement of the position of each electrode for co-registration, the individual head shape was taken into account by the Brainstorm toolbox; thus, the accurate source localization of observed effects should be interpreted with caution. The most important limitation of this study is the small sample size (20 control subjects, 20 MDD subjects). Therefore, the results require replication in an independent dataset. In addition, the design of this study did not allow us to compare gender differences. Future studies may investigate the variants of gender.

5. Conclusions

We proposed an approach combining extended group spatial Fourier ICA and acoustic feature extraction to investigate the group differences in frequency-specific networks under music listening conditions between MDD subjects and healthy

control subjects. We also examined the relationship between depressive symptoms (measured by self-report questionnaire) and frequency-specific patterns. The results were partly in agreement with those reported in earlier literature on MDD using fMRI and MEG/EEG and demonstrated the flexibility of group ICA to study disrupted brain oscillations in psychiatric disorders.

Acknowledgements

This work was supported by the National Natural Science Foundation of China (Grant No. 91748105&81471742), the Fundamental Research Funds for the Central Universities [DUT2019] at Dalian University of Technology in China and a scholarship from China Scholarship Council (Nos. 201600090042 and 201600090043).

References

1. Brookes M. J., Woolrich M., Luckhoo H., Price D., Hale J. R., Stephenson M. C., Barnes G. R., Smith S. M. and Morris P. G. 2011, "Investigating the electrophysiological basis of resting state networks using magnetoencephalography," *Proceedings of the national academy of sciences* **108**, 16783-16788.
2. Damoiseaux J., Rombouts S., Barkhof F., Scheltens P., Stam C., Smith S. M. and Beckmann C. 2006, "Consistent resting-state networks across healthy subjects," *Proceedings of the national academy of sciences* **103**, 13848-13853.
3. Ahmadlou M., Adeli A., Bajo R. and Adeli H. 2014, "Complexity of functional connectivity networks in mild cognitive impairment subjects during a working memory task," *Clinical Neurophysiology* **125**, 694-702.
4. Ahmadlou M. and Adeli H. 2011, "Functional community analysis of brain: A new approach for EEG-based investigation of the brain pathology," *NeuroImage* **58**, 401-408.
5. delEtoile J. and Adeli H. 2017, "Graph theory and brain connectivity in Alzheimer's disease," *The Neuroscientist* **23**, 616-626.
6. Yuvaraj R., Murugappan M., Acharya U. R., Adeli H., Ibrahim N. M. and Mesquita E. 2016, "Brain functional connectivity patterns for emotional state classification in Parkinson's disease patients without dementia," *Behavioural brain research* **298**, 248-260.
7. Ahmadlou M., Adeli H. and Adeli A. 2012, "Fuzzy synchronization likelihood-wavelet methodology for diagnosis of autism spectrum disorder," *Journal of neuroscience methods* **211**, 203-209.
8. Brakowski J., Spinelli S., Dörig N., Bosch O. G., Manoliu A., Holtforth M. G. and Seifritz E. 2017, "Resting state brain network function in major depression–Depression symptomatology, antidepressant treatment effects, future research," *Journal of psychiatric research* **92**, 147-159.
9. Mulders P. C., van Eijndhoven P. F., Schene A. H., Beckmann C. F. and Tendolkar I. 2015, "Resting-state functional connectivity in major depressive disorder: a review," *Neuroscience & Biobehavioral Reviews* **56**, 330-344.
10. Zhu Y., Liu J., Ye C., Mathiak K., Astikainen P., Ristaniemi T. and Cong F. 2020, "Discovering dynamic task-modulated functional networks with specific spectral modes using MEG," *NeuroImage* **218**, 116924.
11. Brookes M. J., Liddle E. B., Hale J. R., Woolrich M. W., Luckhoo H., Liddle P. F. and Morris P. G. 2012, "Task induced modulation of neural oscillations in electrophysiological brain networks," *NeuroImage* **63**, 1918-1930.
12. O'Neill G. C., Tewarie P. K., Colclough G. L., Gascoyne L. E., Hunt B. A. E., Morris P. G., Woolrich M. W. and Brookes M. J. 2017, "Measurement of dynamic task related functional networks using MEG," *NeuroImage* **146**, 667-678.
13. Alluri V., Toiviainen P., Jääskeläinen I. P., Glerean E., Sams M. and Brattico E. 2012, "Large-scale brain networks emerge from dynamic processing of musical timbre, key and rhythm," *NeuroImage* **59**, 3677-3689.
14. Cong F., Phan A. H., Zhao Q.B., Nandi A. K., Alluri V., Toiviainen P., Poikonen H., Huotilainen M., Cichocki, A., Ristaniemi, T. 2012, "Analysis of Ongoing EEG Elicited by Natural Music Stimuli Using Nonnegative Tensor Factorization ", The 2012 European Signal Processing Conference (EUSIPCO-2012), Bucharest, Romania, August 27-31, 2012, pp.494-498.
15. Lankinen K., Smeds E., Tikka P., Pihko E., Hari R. and Koskinen M. 2016, "Haptic contents of a movie dynamically engage the spectator's sensorimotor cortex," *Human brain mapping* **37**, 4061-4068.
16. Wolf D., Mittelberg I., Rekittke L.-M., Bhavsar S., Zvyagintsev M., Haeck A., Klasen M., Cong F. and Mathiak K. 2018, "Interpretation of social interactions: Functional imaging of cognitive-semiotic categories during naturalistic viewing," *Frontiers in human neuroscience* **12**, 296.
17. Zhu Y., Liu J., Mathiak K., Ristaniemi T. and Cong F. 2019, "Deriving electrophysiological brain network connectivity via tensor component analysis during freely listening to music," *IEEE Transactions on Neural Systems and Rehabilitation Engineering* **28**, 409-418.
18. Zhu Y., Liu J., Ristaniemi T. and Cong F. 2020, "Distinct Patterns of Functional Connectivity During the Comprehension of Natural, Narrative Speech," *International journal of neural systems* **30**, 2050007.
19. Cong F., Kalyakin I., Huttunen-Scott T., Li H., Lyytinen H. and Ristaniemi T. 2010, "Single-trial based independent component analysis on mismatch negativity in children," *International journal of neural systems* **20**, 279-292.

20. Cong F., Phan A.-H., Astikainen P., Zhao Q., Wu Q., Hietanen J. K., Ristaniemi T. and Cichocki A. 2013, "Multi-domain feature extraction for small event-related potentials through nonnegative multi-way array decomposition from low dense array EEG," *International journal of neural systems* **23**, 1350006.
21. Jin J., Sellers E. W., Zhou S., Zhang Y., Wang X. and Cichocki A. 2015, "A P300 brain–computer interface based on a modification of the mismatch negativity paradigm," *International journal of neural systems* **25**, 1550011.
22. Zhang Y., Wang Y., Jin J. and Wang X. 2017, "Sparse Bayesian learning for obtaining sparsity of EEG frequency bands based feature vectors in motor imagery classification," *International journal of neural systems* **27**, 1650032.
23. Zhang Y., Zhou G., Jin J., Zhao Q., Wang X. and Cichocki A. 2014, "Aggregation of sparse linear discriminant analyses for event-related potential classification in brain-computer interface," *International journal of neural systems* **24**, 1450003.
24. Jiao Y., Zhang Y., Wang Y., Wang B., Jin J. and Wang X. 2018, "A novel multilayer correlation maximization model for improving CCA-based frequency recognition in SSVEP brain–computer interface," *International journal of neural systems* **28**, 1750039.
25. Sonkusare S., Breakspear M. and Guo C. 2019, "Naturalistic stimuli in neuroscience: Critically acclaimed," *Trends in cognitive sciences **23**, 699-714*.
26. Hasson U., Nir Y., Levy I., Fuhrmann G. and Malach R. 2004, "Intersubject synchronization of cortical activity during natural vision," *science* **303**, 1634-1640.
27. Lankinen K., Saari J., Hari R. and Koskinen M. 2014, "Intersubject consistency of cortical MEG signals during movie viewing," *NeuroImage* **92**, 217-224.
28. Abrams D. A., Ryali S., Chen T., Chordia P., Khouzam A., Levitin D. J. and Menon V. 2013, "Inter-subject synchronization of brain responses during natural music listening," *European Journal of Neuroscience* **37**, 1458-1469.
29. Zhu Y., Zhang C., Poikonen H., Toiviainen P., Huotilainen M., Mathiak K., Ristaniemi T. and Cong F. 2020, "Exploring Frequency-dependent Brain Networks from ongoing EEG using Spatial ICA during music listening," *Brain Topography* **33**, 289-302.
30. Yan C.-G., Chen X., Li L., Castellanos F. X., Bai T.-J., Bo Q.-J., Cao J., Chen G.-M., Chen N.-X. and Chen W. 2019, "Reduced default mode network functional connectivity in patients with recurrent major depressive disorder," *Proceedings of the National Academy of Sciences* **116**, 9078-9083.
31. Pang X., Xu J., Chang Y., Tang D., Zheng Y., Liu Y. and Sun Y. 2014, "Mismatch negativity of sad syllables is absent in patients with major depressive disorder," *PloS one* **9**, e91995.
32. Acharya U. R., Oh S. L., Hagiwara Y., Tan J. H., Adeli H. and Subha D. P. 2018, "Automated EEG-based screening of depression using deep convolutional neural network," *Computer methods and programs in biomedicine* **161**, 103-113.
33. Acharya U. R., Sudarshan V. K., Adeli H., Santhosh J., Koh J. E. and Adeli A. 2015, "Computer-aided diagnosis of depression using EEG signals," *European neurology* **73**, 329-336.
34. Acharya U. R., Sudarshan V. K., Adeli H., Santhosh J., Koh J. E., Puthankatti S. D. and Adeli A. 2015, "A novel depression diagnosis index using nonlinear features in EEG signals," *European neurology* **74**, 79-83.
35. Ahmadlou M., Adeli H. and Adeli A. 2012, "Fractality analysis of frontal brain in major depressive disorder," *International Journal of Psychophysiology* **85**, 206-211.
36. Ahmadlou M., Adeli H. and Adeli A. 2013, "Spatiotemporal analysis of relative convergence of EEGs reveals differences between brain dynamics of depressive women and men," *Clinical EEG and neuroscience* **44**, 175-181.
37. Jiang Y., Duan M., Chen X., Zhang X., Gong J., Dong D., Li H., Yi Q., Wang S. and Wang J. 2019, "Aberrant Prefrontal–Thalamic–Cerebellar Circuit in Schizophrenia and Depression: Evidence From a Possible Causal Connectivity," *International journal of neural systems* **29**, 1850032.
38. Xu J., Wang J., Bai T., Zhang X., Li T., Hu Q., Li H., Zhang L., Wei Q. and Tian Y. 2019, "Electroconvulsive Therapy Induces Cortical Morphological Alterations in Major Depressive Disorder Revealed with Surface-Based Morphometry Analysis," *International journal of neural systems* **29**, 1950005-1950005.
39. Price J. L. and Drevets W. C. 2010, "Neurocircuitry of mood disorders," *Neuropsychopharmacology* **35**, 192.
40. He Y., Lim S., Fortunato S., Sporns O., Zhang L., Qiu J., Xie P. and Zuo X.-N. 2017, "Reconfiguration of Cortical Networks in MDD Uncovered by Multiscale Community Detection with fMRI," *Cerebral Cortex **28**(4), 1383-1395*.
41. Chan M. F., Wong Z. Y. and Thayala N. 2011, "The effectiveness of music listening in reducing depressive symptoms in adults: a systematic review," *Complementary Therapies in Medicine* **19**, 332-348.
42. Hole J., Hirsch M., Ball E. and Meads C. 2015, "Music as an aid for postoperative recovery in adults: a systematic review and meta-analysis," *The Lancet* **386**, 1659-1671.
43. Solanki M. S., Zafar M. and Rastogi R. 2013, "Music as a therapy: role in psychiatry," *Asian Journal of Psychiatry* **6**, 193-199.
44. Mammone N., De Salvo S., Bonanno L., Ieracitano C., Marino S., Marra A., Bramanti A. and Morabito F. C. 2018, "Brain Network Analysis of Compressive Sensed High-Density EEG Signals in AD and MCI Subjects," *IEEE Transactions on Industrial Informatics* **15**, 527-536.
45. Nugent A. C., Robinson S. E., Coppola R., Furey M. L. and Zarate Jr C. A. 2015, "Group differences in MEG-ICA derived resting state networks: application to major depressive disorder," *NeuroImage* **118**, 1-12.
46. Alluri V., Toiviainen P., Jaaskelainen I. P., Glerean E., Sams M. and Brattico E. 2012, "Large-scale brain networks emerge from dynamic processing of musical timbre, key and rhythm," *NeuroImage* **59**, 3677-3689.

47. Cong F., Alluri V., Nandi A. K., Toiviainen P., Fa R., Abu-Jamous B., Gong L., Craenen B. G. W., Poikonen H., Huotilainen M. and Ristaniemi T. 2013, "Linking Brain Responses to Naturalistic Music Through Analysis of Ongoing EEG and Stimulus Features," *IEEE Transactions on Multimedia* **15**, 1060-1069.
48. Delorme A. and Makeig S. 2004, "EEGLAB: an open source toolbox for analysis of single-trial EEG dynamics including independent component analysis," *Journal of neuroscience methods* **134**, 9-21.
49. Olivier Lartillot P. T. 2007, "A Matlab toolbox for musical feature extraction from audio," *International Conference on Digital Audio Effects* **237-244**.
50. Tadel F., Baillet S., Mosher J. C., Pantazis D. and Leahy R. M. 2011, "Brainstorm: a user-friendly application for MEG/EEG analysis," *Computational intelligence and neuroscience* **2011**, 879716.
51. Smith S. M., Fox P. T., Miller K. L., Glahn D. C., Fox P. M., Mackay C. E., Filippini N., Watkins K. E., Toro R. and Laird A. R. 2009, "Correspondence of the brain's functional architecture during activation and rest," *Proceedings of the National Academy of Sciences* **106**, 13040-13045.
52. Kiviniemi V., Starck T., Remes J., Long X., Nikkinen J., Haapea M., Veijola J., Moilanen I., Isohanni M. and Zang Y. F. 2009, "Functional segmentation of the brain cortex using high model order group PICA," *Human brain mapping* **30**, 3865-3886.
53. Kuang L.-D., Lin Q.-H., Gong X.-F., Cong F., Sui J. and Calhoun V. D. 2018, "Model order effects on ICA of resting-state complex-valued fMRI data: Application to schizophrenia," *Journal of neuroscience methods* **304**, 24-38.
54. Allen E. A., Erhardt E. B., Wei Y., Eichele T. and Calhoun V. D. 2012, "Capturing inter-subject variability with group independent component analysis of fMRI data: a simulation study," *NeuroImage* **59**, 4141-4159.
55. Ramkumar P., Parkkonen L., Hari R. and Hyvarinen A. 2012, "Characterization of neuromagnetic brain rhythms over time scales of minutes using spatial independent component analysis," *Human Brain Mapping* **33**, 1648-1662.
56. Ramkumar P., Parkkonen L. and Hyvarinen A. 2014, "Group-level spatial independent component analysis of Fourier envelopes of resting-state MEG data," *NeuroImage* **86**, 480-491.
57. Himberg J., Hyvarinen A. and Esposito F. 2004, "Validating the independent components of neuroimaging time series via clustering and visualization," *NeuroImage* **22**, 1214-1222.
58. Dahne S., Meinecke F. C., Haufe S., Hohne J., Tangermann M., Muller K. R. and Nikulin V. V. 2014, "SPoC: a novel framework for relating the amplitude of neuronal oscillations to behaviorally relevant parameters," *NeuroImage* **86**, 111-122.
59. Morabito C. 2000, "Independent component analysis and feature extraction techniques for NDT data," *Materials evaluation* **58**, 85-92.
60. Nugent A. C., Robinson S. E., Coppola R., Furey M. L. and Zarate C. A., Jr. 2015, "Group differences in MEG-ICA derived resting state networks: Application to major depressive disorder," *NeuroImage* **118**, 1-12.
61. Brakowski J., Spinelli S., Dorig N., Bosch O. G., Manoliu A., Holtforth M. G. and Seifritz E. 2017, "Resting state brain network function in major depression - Depression symptomatology, antidepressant treatment effects, future research," *Journal of psychiatric research* **92**, 147-159.
62. Mulders P. C., van Eijndhoven P. F., Schene A. H., Beckmann C. F. and Tendolkar I. 2015, "Resting-state functional connectivity in major depressive disorder: A review," *Neuroscience & Biobehavioral Reviews* **56**, 330-344.
63. Nugent A. C., Robinson S. E., Coppola R. and Zarate C. A., Jr. 2016, "Preliminary differences in resting state MEG functional connectivity pre- and post-ketamine in major depressive disorder," *Psychiatry Research: Neuroimaging* **254**, 56-66.
64. Wang L., Hermens D. F., Hickie I. B. and Lagopoulos J. 2012, "A systematic review of resting-state functional-MRI studies in major depression," *Journal of affective disorders, 142(1-3), 6-12*.
65. Li Y., Kang C., Wei Z., Qu X., Liu T., Zhou Y. and Hu Y. 2017, "Beta oscillations in major depression - signalling a new cortical circuit for central executive function," *Scientific reports* **7(1)**, 1-15.
66. Fingelkurts A. A., Fingelkurts A. A., Rytsala H., Suominen K., Isometsa E. and Kahkonen S. 2007, "Impaired functional connectivity at EEG alpha and theta frequency bands in major depression," *Human Brain Mapping* **28**, 247-61.
67. Fingelkurts A. A. and Fingelkurts A. A. 2015, "Altered structure of dynamic electroencephalogram oscillatory pattern in major depression," *Biological psychiatry* **77**, 1050-1060.
68. Cong F., Lin Q.-H., Kuang L.-D., Gong X.-F., Astikainen P. and Ristaniemi T. 2015, "Tensor decomposition of EEG signals: a brief review," *Journal of neuroscience methods* **248**, 59-69.
69. Wang D., Zhu Y., Ristaniemi T. and Cong F. 2018, "Extracting multi-mode ERP features using fifth-order nonnegative tensor decomposition," *Journal of neuroscience methods* **308**, 240-247.
70. Zhu Y., Li X., Ristaniemi T. and Cong F. 2019, "Measuring the Task Induced Oscillatory Brain Activity Using Tensor Decomposition," in ICASSP 2019-2019 IEEE International Conference on Acoustics, Speech and Signal Processing (ICASSP) (pp. 8593-8597). IEEE.